ENGINEERING Environment
2026, 20(5): 80 https://doi.org/10.1007/s11783-026-2180-2

REVIEW ARTICLE

A review on characterizing atmospheric ultrafine particles

Minghao Wang[1], Michel Attoui ✉ [2], Min Hu[3], Jingkun Jiang ✉ [1]

1. State Key Laboratory of Regional Environment and Sustainability, School of Environment, Tsinghua University, Beijing 100084, China
2. LISA, Université Paris Est Créteil; Université Paris Cité; CNRS, Créteil F-94010, France
3. State Key Laboratory of Regional Environment and Sustainability, International Joint Research Center for Atmospheric Research (IJRC), College of Environmental Sciences and Engineering, Peking University, Beijing 100871, China

HIGHLIGHTS

- Characterization of UFPs requires developing new techniques.
- Standardized protocols ensure data comparability across atmospheres.
- Properties of UFPs beyond number concentration require further investigation.
- Data-driven machine learning models can bridge network monitoring gaps.

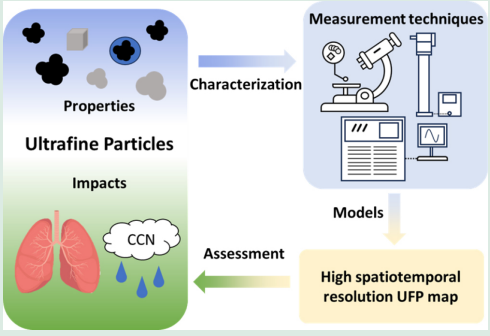

ABSTRACT: Atmospheric ultrafine particles (UFPs) dominate the number concentration of ambient particulate matters and have potentially high health effects. Their ultrafine size (< 100 nm) results in extremely low mass and weak light-scattering signals, thereby limiting the applicability of measurement techniques used for fine particles ($PM_{2.5}$). This review synthesizes the existing techniques developed to characterize the complex properties of UFPs, including concentration, size distribution, chemical composition, and morphology. Despite existing UFP field observations, challenges remain in developing a comprehensive understanding of global UFP properties. Inconsistencies in instrumentation and critical parameters across different campaigns hinder data comparability, underscoring the need for standardized measurement protocols. Furthermore, current UFP monitoring networks primarily focus on concentration and size distribution, with other key properties, like chemical composition, remaining largely outside routine monitoring and limited to dedicated research campaigns or supersites. Machine learning approaches offer a promising avenue to integrate independent studies, enabling a more comprehensive understanding of global UFP properties. Such comprehensive characterization is essential for accurately assessing UFP exposure risks and climate impacts. These insights are urgently needed to strengthen existing particle-number-concentration-based regulatory frameworks and develop more effective air quality guidelines and emission control strategies.

KEYWORDS: Ultrafine particle, Size distribution, Measurement techniques, *in-situ* observation, Modeling

✉ Corresponding authors. E-mails: attoui@u-pec.fr (M. Attoui); jiangjk@tsinghua.edu.cn (J. Jiang)

Article history: Received 9 January 2026, Revised 18 April 2026, Accepted 20 April 2026, Available online 12 May 2026

Special issue—Atmospheric ultrafine particles (Guest editors: Kebin He, Lidia Morawska, Guangjie Zheng & Xiaoxiao Li)

1 Introduction

Although ultrafine particles (UFPs) are a subset of $PM_{2.5}$, conventional $PM_{2.5}$ measurement methods are often ineffective in characterizing these aerosols with diameters below 100 nm. As shown in Fig. 1(a), UFPs dominate particle number concentration (PNC) yet contribute negligibly to mass concentration (PMC). Consequently, PNC is a more suitable metric for quantifying UFPs. Moreover, their weak light-scattering intensity, depicted in Fig. 1(b), renders conventional optical techniques ineffective for UFP investigation (Vasilatou et al., 2021). Since these aerosols exert both climate forcing and human health effects (Chalupa et al., 2004; Kuula et al., 2020; Moreno-Ríos et al., 2022), it is crucial to develop and deploy advanced techniques for effective atmospheric UFP observation.

Currently, there is a growing international consensus on the need to monitor PNC, with specific observational requirements proposed to support health risk assessment. The World Health Organization (WHO) recommends continuous measurement of particle number size distribution (PNSD) above 10 nm at ambient monitoring stations (WHO, 2021). The European Union mandates that member states establish sampling points to monitor potential high UFP levels for every five million residents, and designate a monitoring supersite for background levels of urban air pollutants, including UFPs, for every ten million residents (European Parliament & Council of the European Union, 2024). Existing aerosol monitoring networks provide a fundamental infrastructure for observing UFPs (Birmili et al., 2009; Kivekäs et al., 2009; Li et al., 2024). Moreover, mobile monitoring and numerical modeling provide distributions of PNC with high spatial resolution for assessing local emissions and population exposure (Steffens et al., 2017; Lloyd et al., 2024).

Beyond PNC and PNSD, a comprehensive investigation into properties of ambient UFPs is necessary for the accurate assessment of their exposure risks and environmental impacts. These properties include chemical composition, surface area, hygro-scopicity, morphology, and density. Measuring key chemical components of UFPs is directly relevant to both source identification and toxicity analysis (Pietrogrande et al., 2022; Li et al., 2023b). Particle surface area has been suggested as one of the most relevant metrics for evaluating health impacts (Schmid and Stoeger, 2016). Measurements of particle density and morphology are critical for refining lung deposition modeling based solely on diameters (DeCarlo et al., 2004). Measurements of particle hygroscopicity are essential for accurately characterizing climate-relevant effects of UFPs, such as contributing cloud conden-sation nuclei (Dutta et al., 2023).

To date, numerous studies have reported on the principles and technological developments of aerosol measurement (McMurry, 2000b; Zhang and Han, 2025a, 2025b). Morawska et al. (2009) comprehensively reviewed early UFP measurement techniques. Lei et al. (2024) compiled current analytical techniques for UFP and reviewed their applications in assessing

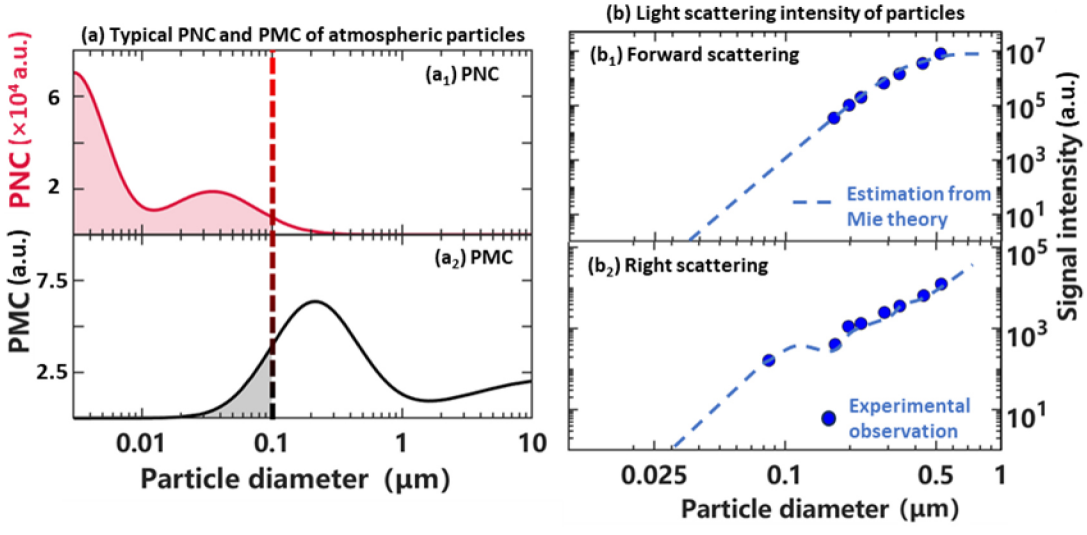

Fig. 1 The (a) concentration and (b) light scattering characteristics of particles with varying size (Zarrin et al., 1987; Seinfeld and Pandis, 2016).

UFP health and climate impacts. Li et al. (2023a) reviewed the techniques for online analysis of UFP chemical composition and the challenges faced. This paper further reports on recent advances in measurement techniques. It also reviews current methods for characterizing atmospheric UFPs, identifies remaining challenges, and discusses potential solutions involving machine learning to develop a comprehensive understanding of atmospheric UFPs.

2 Measuring properties of UFPs

2.1 Particle number concentration

PNC is a key regulatory parameter for particle emissions, and can be measured by electrical methods and optical counting (Flagan, 1998; Abdillah and Wang, 2023). In electrical approaches, PNC is measured by detecting the current generated by charged particles within a Faraday cup. The accuracy of this method fundamentally depends on an accurately quantified particle charging state, which is highly variable and difficult to determine, as it hinges on the particles, the ambient conditions, and the charger itself (Wiedensohler et al., 1986; Tigges et al., 2015). These limitations may lead to measurement uncertainty compared to other methods (Fierz, 2011).

Optical detection method counts particles by directly capturing their light scattering signals, typically covering a measurable size range of 0.3–10 μm (Iida and Sakurai, 2018). By coupling particle condensation growth technology, a condensation particle counter (CPC) can detect nanoparticles (McMurry, 2000a). Adjusting the temperature difference between the saturator and condenser sections (Baltzer et al., 2014; Attoui, 2018), and employing working fluids with high surface tension and low vapor pressure (Iida et al., 2009; Jiang et al., 2011) facilitate the reduction of the minimum detectable size to ~1 nm. Recently, a convertible CPC has been developed to accommodate different working fluids, thereby improving operational flexibility (Li et al., 2025). Optimizing the optical and circuit designs to minimize particle pulse width can mitigate the coincidence and shielding effects that cause PNC underestimation at high concentrations, thus raising the CPC's upper detection limit (Wang et al., 2020).

2.2 Particle number size distribution

PNSD can be used to investigate atmospheric physico-chemical processes (Deng et al., 2020), such as new particle formation (NPF) and growth due to condensation and heterogeneous reactions, as well as for source apportionment (Beddows et al., 2009). Particle size can be characterized by different metrics, such as aerodynamic diameter and mobility diameter. These metrics not only differ in their measurement principles, but also often yield distinct values for the same particle (McMurry, 2000b).

Aerodynamic diameter determines particle aerodynamic behavior, such as deposition in the human respiratory tract (Bartol et al., 2024). Impactors separate and sample UFPs of different aerodynamic sizes based on inertia effects (Sardar et al., 2005; Zahir et al., 2025). Recently, the aerodynamic aerosol classifier (AAC) was developed. This instrument classifies particles by aerodynamic diameter based on the equilibrium between centrifugal force and drag force in a rotating flow field (Tavakoli and Olfert, 2013). Currently, commercial AAC instruments can classify particles with aerodynamic diameters down to ~25 nm (Pongetti et al., 2022).

Electrical mobility, defined as the terminal velocity of a particle in unit electric field, is the key metric utilized in mobility size classifiers (Hinds and Zhu, 2022). Common instruments, such as the Differential Mobility Analyzer (DMA), classify particles by varying the electric field strength. Only charged particles within a specific mobility diameter range can reach the sampling slit of the DMA for a given voltage setting, and be counted. These counts are then corrected for particle charging fraction, CPC detection efficiency, system transmission efficiency, and DMA transfer function to derive the size-resolved PNC. The Scanning Mobility Particle Sizer (SMPS) is the commonly used instrument designed based on this principle for measuring PNSD. A typical SMPS operates in the size range of approximately 10–1000 nm with a time resolution of 1–2 minutes. Additionally, the Fast Mobility Particle Sizer (FMPS) employs an integrated multi-channel electrometer electrode array to simultaneously measure currents from charged particles of different sizes, achieving a time resolution of 1s across a size range of 5.6–560 nm (Tammet et al., 2002). To observe nanometer-sized UFPs or molecular clusters, specially designed instruments are required. Nano-DMA (1–150 nm) or the Neutral Aerosol Ion Spectrometer (NAIS) (0.8–40 nm) can be used for mobility analysis (Chen et al., 1998; Manninen et al., 2016; Cai et al., 2017).

Assuming fixed particle charging fractions are widely used for PNSD inversion but may introduce uncertainties (Fuchs, 1963; Wiedensohler, 1988;

Wiedensohler et al., 2012). This is because the actual charging process is dynamic, not steady-state, leading to significant inaccuracy in charge fraction estimation (Jiang et al., 2014). Since the relative differences in positive and negative ion characteristics are critical factors influencing the bipolar charging fractions (Jiang et al., 2014; Tigges et al., 2015), both positively and negatively charged particles are recommended to be accounted for during the measurement and the data inversion (Jiang et al., 2014). Thus, one can achieve true particle charging fractions in real-time and reconstructs the original PNSD based on the combined proportions of positively and negatively charged particles (Gunn and Woessner, 1956; Chen and Jiang, 2018; Chen et al., 2018). This approach not only significantly improves inversion accuracy, but also enhances the robustness of measurements against variations in aerosol charging states (Li et al., 2022b, 2024).

2.3 Surface area and density

Surface area, a proxy for the chemical reactivity of particles, can be derived from the measured diameter by assuming sphericity (Gong et al., 2019). Oftentimes, however, particles are not spherical (Lv and Zhao, 2025). This morphological deviation becomes particularly critical in studies of aerosol dynamics and pathological investigations (Voth and Soldati, 2017; Lv et al., 2024), necessitating more accurate characterization methods. Different measurement principles and objectives lead to varying definitions of particle surface area. The Brunauer-Emmett-Teller (BET) surface area, determined through low-temperature nitrogen adsorption, characterizes the total physical specific surface area including pore structures (Haul, 1982). The active surface area, quantified by the adsorption kinetics of radiolabeled tracer molecules, reflects the effective interface participating in specific chemical reactions (Konstandopoulos et al., 2004). In health effect studies, the lung deposited surface area (LDSA) serves as an indicator of particle reactivity and lung interaction potential (Edebeli et al., 2023). It can be directly measured by electrical current detection following corona charging under simulated respiratory conditions (Fissan et al., 2007), or derived by applying a weighting integration to the PNSD based on established alveolar deposition fraction curves (Bair, 1992).

Particle density, defined as true or effective, serves as the bridge between mobility and aerodynamic diameter. The true density is determined based on the fundamental mass-to-volume relationship. The volume of particles is typically measured via displacement by inert gas (Bartley et al., 2020). This volume is combined with mass measurement to obtain the true density. This method significantly eliminates the influence of particle morphology on the volume measurement, providing the intrinsic material density. The measurement of effective density is commonly based on two methodological approaches. The first approach couples a Centrifugal Particle Mass Analyzer (CPMA) in tandem with a DMA to classify the mass of mobility-selected particles. With particle volume estimated from the mobility diameter, the effective density can be calculated (Gu et al., 2025). The second approach infers particle density by combining measurements of aerodynamic diameter and mobility diameter (Hering and Stolzenburg, 1995).

2.4 Morphology

The weak light scattering of UFPs falls below the detection limit of conventional optical instruments designed for morphological analysis (Kaye et al., 1996; Burton et al., 2012; Ding et al., 2016). Consequently, morphological analysis of UFP samples is typically conducted using off-line electron microscopy (Dong et al., 2019; Kirpes et al., 2020). Based on analysis of high-resolution particle images, morphology can be characterized either through direct description or calculating specific shape factors.

While direct morphological description accurately captures features, its lack of quantifiable metrics hinders integrating them into aerosol dynamics analysis. Lv and Zhao have summarized shape factors used to quantify particle morphology (Lv and Zhao, 2025). Among these, sphericity is often used, defined as the ratio of the surface area of a sphere with the same volume as the particle to the actual surface area of the particle (Wadell, 1932). This metric effectively quantifies the deviation of a particle's shape from a perfect sphere and has employed in simulations of the aerodynamic behavior of non-spherical particles.

2.5 Chemical components

Particle compositional information serves as a tracer for sources and a predictor of toxicity. Well-established laboratory analytical procedures provide comprehensive chemical characterization for aerosol samples (Morawska et al., 2009). However, these offline methods cannot resolve the rapid atmospheric aging of UFPs (Li et al., 2022a).

Online analytical techniques vary according to the targeted level of detail in chemical characterization. For

specific components analysis, typical instrument combinations are often required. For example, ultrafine black carbon (BC) analysis relies on a BC detector coupled with a DMA (Ning et al., 2013). By inserting a thermodenuder between tandem DMAs, the volatility distribution of aerosol components can be determined from particle size shrinkage after thermal desorption (Rader and McMurry, 1986; Sakurai et al., 2005; Oxford et al., 2019). Based on this information, the aging state of ambient aerosols and the mixing state evolution of newly formed particles can be further analyzed. (Chen et al., 2022; Wu et al., 2023). Further chemical characterization requires mass spectrometric techniques. For instance, high-resolution time-of-flight aerosol mass spectrometer (HR-ToF-AMS) can quantitatively resolve major species including sulfate, nitrate, and ammonium, as well as organics and their elemental composition (Hu et al., 2016). For detailed time-resolved near-molecular-level characterization, the thermal desorption-chemical ionization mass spectrometer (TDCIMS) is a commonly used technique, owing to its relatively low fragmentation and high sensitivity (Smith et al., 2004). A dedicated review of efforts to advance real-time analysis of atmospheric UFP molecular composition is available in the literature (Li et al., 2023a).

2.6 Hygroscopicity

Conventional SMPS measurements often lack information on hygroscopic growth due to pre-drying, leading to discrepancies between measurement and reality (Fajardo et al., 2016; WMO, 2016). Hygroscopicity measurements are thereby critical for assessing hygroscopic growth, which directly influences particle's climate and health effects (Vu et al., 2015; Jung et al., 2023a). By classifying monodisperse particles using a DMA and monitoring their size or state after hygroscopic growth, the hygroscopic growth factor (GF) and hygroscopicity parameter (κ) can be determined (Rader and McMurry, 1986).

An alternative approach derives particle's hygroscopicity from its chemical composition. By applying the Zdanovskii-Stokes-Robinson (ZSR) rule, the overall hygroscopicity parameter κ can be estimated as the mass-weighted average of the κ of individual components (Zdanovskii, 1936; Stokes and Robinson, 1966). For instance, Zhao et al. determined the size-resolved chemical composition of particles (10 nm–18 μm) and well derived κ values based on ZSR rule (Zhao et al., 2020). Conversely, based on the hygroscopicity parameter κ and the ZSR rule, the volume fractions of major chemical species can be estimated as well (Aklilu and Mozurkewich, 2004). When combined with volatility analysis, the internal mixing state of particles can be further analyzed (Villani et al., 2008).

2.7 Toxicity

Oxidative stress, resulting from reactive oxygen species (ROS) generated by redox-active components, is a pivotal toxicological mechanism for aerosol health effects (Jiang et al., 2008; Gao et al., 2020). The ROS-generating capacity is defined as oxidative potential (OP), quantified via acellular assays such as the dithiothreitol (DTT) method, which measures OP by the DTT consumption rate in simulated lung fluid (Kurihara et al., 2022). Given the abundance of redox-active constituents in UFPs, OP is likely key to understanding UFPs health effects (Chen et al., 2016).

While mass-normalized OP assays provide valuable insights into the intrinsic toxicity of UFP compared to $PM_{2.5}$ (Jeng, 2010), they cannot fully address the paradox of how such low mass concentrations exert significant adverse health effects. Resolving this question requires a more systematic, biologically grounded approach. *In vivo* studies using animal models expose subjects to UFPs via direct inhalation or systemic injection, inducing biological outcomes and elucidating pathogenic pathways (Farina et al., 2019; Saleh et al., 2019), followed by integrated analysis of physiological parameters and target organ histopathology. However, the translational applicability of these studies faces several inherent limitations, including variability in exposure conditions and fundamental physiological disparities between animal models and humans (Jiang et al., 2009).

3 Characterizing atmospheric UFPs

UFPs exhibit high spatial and temporal variability, making long-term multi-site observations essential for characterizing their regional distribution. However, current long-term UFP monitoring networks primarily focus on PNC and PNSD. Chemical compositional analysis largely relies on offline analysis or short-term campaigns (Nordmann, 2009; Crenn et al., 2015). For other properties, such as hygroscopicity, our understanding relies on historical data compiled from multiple independent studies (Zou et al., 2025). Given that methods for comprehensively characterizing UFP properties remain under development, this review

focuses specifically on techniques for characterizing PNC and PNSD.

As shown in Fig. 2, while network monitoring provides long-term PNC data over large regions, it lacks the spatial detail to resolve local variations. Conversely, mobile platforms capture PNC at high spatial-resolution, but are confined to limited areas. Combining with other simultaneous observation, such as ancillary pollutants and meteorology, these results can be further used to establish predictive models, enabling high spatiotemporal resolution (e.g., ~1 km and ~1h) mapping of UFP.

3.1 From fixed measurements to network monitoring

As summarized in Table 1, the particle size ranges measured vary substantially across different UFP monitoring networks, with inconsistencies also observed between sites within the same network. Although a lower size limit of 10 nm is recommended (WHO, 2021), there is no broad scientific consensus on this value, which partially explains the observed inconsistencies. Nevertheless, this significantly compromises the data comparability across various sites (e.g., PNC varies significantly with the lower size limit). While lognormal fitting can estimate PNSD below the instrumental lower detection limit (Whitby, 1978), such extrapolation may substantially underestimate particle number concentrations during NPF events. For specific research needs, the Global Atmosphere Watch (GAW) program recommends a detection limit of 3 nm (WMO, 2016). To ensure data comparability, a 10 nm lower size limit should be applied as a minimum requirement. This aligns with conventional SMPS capabilities.

3.2 Mobile observation of UFPs

By assigning data to short segments (typically 100 m in length), mobile observation can generate high-spatial-resolution PNC maps along driving routes (Kerckhoffs et al., 2021; Doubleday et al., 2023). This approach is particularly valuable in complex urban areas, allowing detailed assessment of UFP impacts on ambient air quality and population exposure (Weichenthal et al., 2014).

Mobile measurements require high time resolution, thereby limiting instrument selection. Since a vehicle passes a 100-m segment in only a few seconds, the instrument must complete multiple measurements within this brief time window to ensure data robustness. Consequently, conventional SMPS, with a minute-level time resolution, is unsuitable for mobile PNSD measurement. Alternatively, FMPS have been employed to obtain high time resolution PNSD data under these conditions (Weimer et al., 2009). Besides, many studies focus solely on measuring PNC during mobile surveys (Gani et al., 2021; Kerckhoffs et al., 2021). Portable instruments, such as the Discmini or P-Trak, are another common choice for particle counting, as their compact and low-power consumption is well-suited to the constraints of mobile platforms (Doubleday et al., 2023; Lloyd et al., 2023). In contrast, the SMPS is feasible for PNSD measurements in aerial observations (Wehner et al., 2010; Liu et al., 2024). The platform's ability to hover for extended periods accommodates the longer scan time of the SMPS.

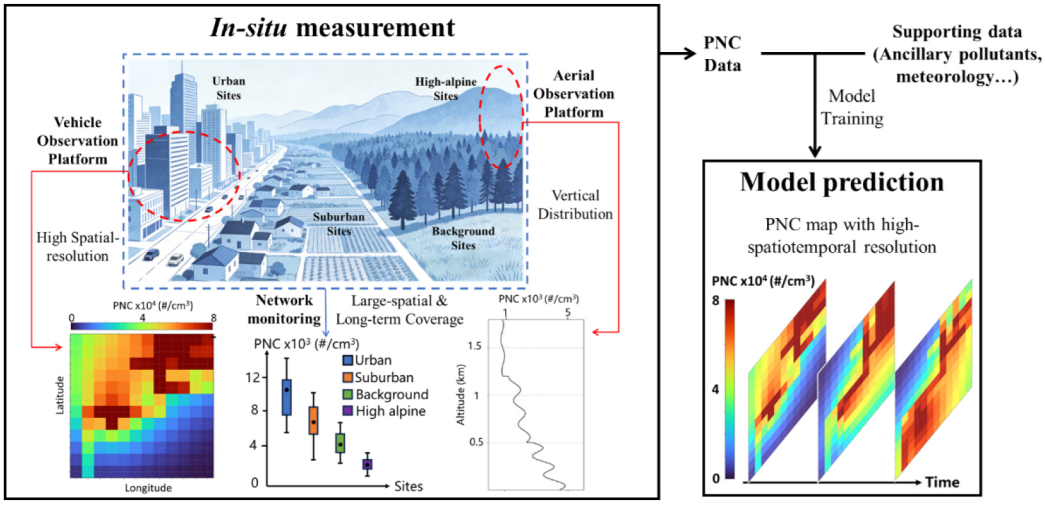

Fig. 2 Methodologies for ambient UFP characterization.

Table 1 Comparison between different ambient UFP network monitoring

Countries/Regions	Network	Periods	Station types and amounts					Measured objects
			RS	UB	SUB	RB	MT	
Germany (Sun et al., 2019)	German UltrafineAerosol Network (GUAN)	2009–2018	3	8	/	3	3	PNC and PNSD from 5–14 nm to 750–800 nm; Black carbon;
Europe (Garcia-Marlès et al., 2024)	Research Infrastructures Services Reinforcing Air Quality Monitoring Networks (RI-URBANs)	2009–2019	6	15	4	1	/	PNC and PNSD from 10–17 nm to 478.3–800 nm; Ancillary pollutants
USA (Andrews et al., 2019)	Federated Aerosol Network (FAN)	Before 2016	28 sites in total					PNC; Black carbon
China (Li et al., 2024)	A bipolar SMPS network	2023–2024	/	3	3	/	/	PNC and PNSD from 10–13 nm to 700 nm

Note: RS: Road Side; UB: Urban Background; SUB: Suburban Background; RB: Regional Background; MT: Mountain.

3.3 From *in-situ* measurements to regional UFP mapping

Statistical relationships between PNC and influencing factors can be utilized to build predictive models for regional UFP mapping (Crippa et al., 2013; Reggente et al., 2014). Among these, Land Use Regression (LUR) modeling is widely used, as comprehensively reviewed by Hoek et al (Hoek et al., 2008). However, developing robust models requires substantial input data, which is often obtained through resource-intensive mobile monitoring campaigns or short-term measurements at a large number of sites (Kerckhoffs et al., 2016, 2017; Jones et al., 2020).

The advancement of machine learning (ML) technology has further propelled the development of predictive models. As shown in Table 2, ML models generally perform well in predicting PNC across various atmospheres, as indicated by high coefficients of determination (R^2). Vachon et al. reported that ML models, especially tree-based models, generally outperform conventional statistical models on the same dataset (Vachon et al., 2024a, 2024b).

A striking inconsistency exists in the literature regarding the selection of key predictors for ML-based UFP models. Jung et al. identified "surface pressure" and "distance to road" as the most important predictors for modelling UFP distribution in central Taiwan, China (Jung et al., 2023b). Xu et al reported NO_2 as the most important predictor for modeling in Toronto (Xu et al., 2022). While such discrepancies could be partly attributed to differences in UFP observation methods, they strongly indicate that the relevance and predictive power of specific predictors are highly location-dependent. Therefore, systematic investigation into governing parameters across diverse environments is needed to develop models that are both robust and parsimonious.

Existing ML prediction models primarily use PNC as the outcome variable, often overlooking PNSD. While these models demonstrate reasonable performance over long temporal scales, their predictive accuracy deteriorates significantly for short-term PNC variations, such as predicting daily-average value (Rahman et al., 2020; Jianyao et al., 2025). The underlying drivers for increased PNC can vary substantially across different size ranges (Beddows et al., 2009). A generalized parameterization of the relationship between total PNC and predictors may fail to capture these distinct dynamics, leading to inaccuracies in short-term forecasts. Rahman et al. reported considerable variation in the importance of predictors when modeling PNC for different size ranges (Rahman et al., 2020), thereby recommending the disaggregation of total PNC into its modal components for model training and prediction purposes.

4 Future outlook

While extensive worldwide monitoring campaigns for PNC and PNSD have provided a good data foundation for training ML models, the poor comparability of data across different campaigns poses a latent risk of introducing hidden biases that undermine model robustness over large scales. In addition to the varying measured size ranges mentioned in Section 3.1, PNC readings from the Discmini, commonly used in mobile monitoring, can be 10%–20% lower than SMPS (Fierz et al., 2011; Mills et al., 2013). This deviation can remain hidden during model evaluation, as the "ground truth" is unavailable for validation. To improve dataset accuracy beyond periodical instrument calibration and inter-instrument comparison, Wiedensohler et al. (2012, 2018) recommended establishing technical standards for SMPS measurements, along with data protocols that ensure traceability throughout the data inversion. These harmonization efforts, however, require updates to accommodate new progresses that replace unrealistic

Table 2 Summary of regional UFP PNC distribution prediction by machine learning

Studied region (estimated area)	UFP data sources	Predictors	Targeted variables (Resolution)	Model performance	Ref.
Quebec, Canada (372 km^2)	Mobile observation (2019.6–2020.6, Discmini)	Land use; Traffic; Topography; Emissions inventories; Meteorology	PNC (Daily & Annual)	R^2 = 0.82–0.86	Vachon et al., 2024a
Central Taiwan, China (7837 km^2)	Fixed monitoring from 6 sites (2008–2010, 2017.9–2021.8, SMPS)	Ancillary pollutants; Meteorology; Land use; Topography	PNC (Seasonal)	R^2 = 0.77–0.78	Jung et al., 2023b
Toronto, Canada (630 km^2)	Mobile observation (2020.8–2021.8, Discmini)	Traffic; Meteorology; Land use; Time	PNC	R^2 = 0.73	Xu et al., 2022
Netherland (41526 km^2)	Mobile observation (14 d, CPC) and Fixed monitoring data from literature	Traffic; Land use; Population	PNC	R^2 = 0.34–0.52	Kerckhoffs et al., 2021
Switzerland (41290 km^2)	Fixed monitoring from 5 sites (2016–2019, 2022, from Swiss National Air Pollution Monitoring Network)	Traffic; Ancillary pollutants; Meteorology;	PNC (Hourly, Daily, Weekly, & Monthly)	R^2 = 0.76–0.91	Jianyao et al., 2025
Global wide	EBAS, NOAA Global Monitoring Laboratory, and other literatures	Population; NO_2 and $PM_{2.5}$; Emissions inventories; Traffic; Meteorology	PNC (Annual)	R^2 = 0.77–0.91	Georgiades et al., 2025
Brisbane Metropolitan Area, Australia (1550 km^2)	Fixed monitoring from 30 sites (2010.10–2012.12, SMPS)	Traffic; Land use; Population; Meteorology; Topography	PNC in 3 size ranges (Hourly)	R^2 = 0.21–0.88	Rahman et al., 2020
Taichung, China (2214 km^2)	Fixed monitoring from 1 site (2018.10–2023.7, SMPS)	Meteorology; Time; Temporal trend	PNC in 4 modes	R^2 = 0.53–0.85	Lin et al., 2025

fixed charge fractions with dynamic charge fractions. It has been demonstrated that dynamic charge fractions can be continuously revealed and used for SMPS data inversion (Li et al., 2022b, 2024).

The WHO recommends defining low PNC as <1000 particles/cm^3 (24-h mean) and high PNC as >10000 particles/cm^3 (24-h mean) to guide decisions on the priorities of UFP source emission control (WHO, 2021). However, even in clean region, elevated PNC levels can also arise from NPF (Venzac et al., 2008; Cai et al., 2018). To inform evidence-based regulation, it is essential to comprehensively characterize UFPs across different environments including PNSD and chemical composition (Ye et al., 2020). Although current research on UFP properties beyond PNSD remains spatially and temporally limited (Air Quality Expert Group, 2018), the accumulation of long-term data and advances in ML offer promising pathways to overcome these barriers. Using meteorological parameters and ancillary pollutants as predictors, ML has been successfully applied to predict long-term variations in $PM_{2.5}$ chemical components (Lv et al., 2021). Given the strong link between UFP size and its sources, incorporating PNSD as an additional predictor into such models could further enhance their robustness. This would enable the extraction of long-term spatial patterns for properties, such as chemical composition, from existing PNSD results. Such integration across different campaigns underscores the need for standardized measurement protocols for UFP properties beyond PNSD, as well as for systematic inter-instrument comparisons, which has been highlighted by well-recognized instrumental discrepancies in mass spectrometry (Riva et al., 2019). Ultimately, comprehensive UFP characterization, coupled with in-depth analyses, such as lung deposition modeling and toxicological studies, can elucidate the exposure risks associated with specific size distributions and chemical components, thereby supporting the development of targeted air quality and emission control policies.

CRediT Authorship Contribution Statement

Minghao Wang: Conceptualization, Methodology, Investigation, Data curation, Formal analysis, Visualization, Writing-original draft, Writing-review & editing; **Michel Attoui:** Conceptualization, Methodology, Investigation, Formal analysis, Supervision, Writing-review & editing; **Min Hu:** Conceptualization, Methodology, Investigation, Formal analysis, Funding acquisition, Project administration; Supervision, Resources, Writing-review & editing; **Jingkun Jiang:** Conceptualization, Methodology, Investigation, Data curation, Formal analysis, Visualization, Funding acquisition, Project administration; Supervision, Resources, Writing-original draft, Writing-review & editing.

Conflicts of Interest The authors declare that the research was conducted in the absence of any commercial or financial relationships that could be construed as a potential conflict of interest.

Acknowledgements This work was supported by Jing-Jin-Ji Regional Integrated Environmental Improvement-National Science and Technology Major Project of Ministry of Ecology and Environment of China (No. 2025ZD1201100) and the Special Fund of State Key laboratory of Regional Environment and Sustainability (No. 25L01RES).

References

Abdillah S F I, Wang Y F (2023). Ambient ultrafine particle ($PM_{0.1}$): sources, characteristics, measurements and exposure implications on human health. Environmental Research, 218: 115061

Air Quality Expert Group (2018). Ultrafine Particles (UFP) in the UK. London: Department for Environment, Food and Rural Affairs

Aklilu Y A, Mozurkewich M (2004). Determination of external and internal mixing of organic and inorganic aerosol components from hygroscopic properties of submicrometer particles during a field study in the lower fraser valley. Aerosol Science and Technology, 38(2): 140–154

Andrews E, Sheridan P J, Ogren J A, Hageman D, Jefferson A, Wendell J, Alástuey A, Alados-Arboledas L, Bergin M, Ealo M, et al. (2019). Overview of the NOAA/ESRL federated aerosol network. Bulletin of the American Meteorological Society, 100(1): 123–135

ANSYS Inc (2021). ANSYS Fluent 2021 R1. Canonsburg, PA, USA

Attoui M (2018). Activation of sub 2 nm singly charged particles with butanol vapors in a boosted 3776 TSI CPC. Journal of Aerosol Science, 126: 47–57

Bair W J (1992). The Revised International Commission on Radiological Protection (ICRP) dosimetric model for the human respiratory tract. Washington: U.S. Department of Energy

Baltzer S, Onel S, Weiss M, Seipenbusch M (2014). Counting efficiency measurements for a new condensation particle counter. Journal of Aerosol Science, 70: 11–14

Bartley P C, Amoozegar A, Fonteno W C, Jackson B E (2020). Particle density of substrate components measured by gas pycnometer. Acta Horticulturae, 1273: 17–22

Bartol I R, Graffigna Palomba M S, Tano M E, Dewji S A (2024). Computational multiphysics modeling of radioactive aerosol deposition in diverse human respiratory tract geometries. Communications Engineering, 3(1): 152

Beddows D C S, Dall'osto M, Harrison R M (2009). Cluster analysis of rural, urban, and curbside atmospheric particle size data. Environmental Science & Technology, 43(13): 4694–4700

Birmili W, Ries L, Sohmer R, Anastou A, Sonntag A, Koenig K, Levin I (2009). Fine and ultrafine aerosol particles at the GAW station Schneefernerhaus/Zugspitze. Gefahrstoffe, Reinhaltung der Luft / Air Quality Control, 69(1−2): 31–35

Burton S P, Ferrare R A, Hostetler C A, Hair J W, Rogers R R, Obland M D, Butler C F, Cook A L, Harper D B, Froyd K D (2012). Aerosol classification using airborne High Spectral Resolution Lidar measurements-methodology and examples. Atmospheric Measurement Techniques, 5(1): 73–98

Cai R L, Chandra I, Yang D S, Yao L, Fu Y Y, Li X X, Lu Y Q, Luo L, Hao J M, Ma Y, et al. (2018). Estimating the influence of transport on aerosol size distributions during new particle formation events. Atmospheric Chemistry and Physics, 18(22): 16587–16599

Cai R L, Chen D R, Hao J M, Jiang J K (2017). A miniature cylindrical differential mobility analyzer for sub-3 nm particle sizing. Journal of Aerosol Science, 106: 111–119

Chalupa D C, Morrow P E, Oberdörster G, Utell M J, Frampton M W (2004). Ultrafine particle deposition in subjects with asthma. Environmental Health Perspectives, 112(8): 879–882

Chen D R, Pui D Y H, Hummes D, Fissan H, Quant F R, Sem G J (1998). Design and evaluation of a nanometer aerosol differential mobility analyzer (Nano-DMA). Journal of Aerosol Science, 29(5−6): 497–509

Chen L, Zhang F, Collins D, Ren J Y, Liu J Y, Jiang S H, Li Z Q (2022). Characterizing the volatility and mixing state of ambient fine particles in the summer and winter of urban Beijing. Atmospheric Chemistry and Physics, 22(4): 2293–2307

Chen R, Hu B, Liu Y, Xu J X, Yang G S, Xu D D, Chen C Y (2016). Beyond $PM_{2.5}$: the role of ultrafine particles on adverse health effects of air pollution. Biochimica et Biophysica Acta (BBA) - General Subjects, 1860(12): 2844–2855

Chen X T, Jiang J K (2018). Retrieving the ion mobility ratio and aerosol charge fractions for a neutralizer in real-world applications. Aerosol Science and Technology, 52(10): 1145–1155

Chen X T, McMurry P H, Jiang J K (2018). Stationary characteristics in bipolar diffusion charging of aerosols: improving the performance of electrical mobility size spectrometers. Aerosol Science and Technology, 52(8): 809–813

Crenn V, Sciare J, Croteau P L, Verlhac S, Fröhlich R, Belis C A, Aas W, Äijälä M, Alastuey A, Artiñano B, et al. (2015). ACTRIS ACSM intercomparison – Part 1: reproducibility of concentration and fragment results from 13 individual Quadrupole Aerosol Chemical Speciation Monitors (Q-ACSM) and consistency with co-located instruments. Atmospheric Measurement Techniques, 8(12): 5063–5087

Crippa P, Spracklen D, Pryor S C (2013). Satellite-derived estimates of ultrafine particle concentrations over eastern North America. Journal of Geophysical Research: Atmospheres, 118(17): 9968–9981

DeCarlo P F, Slowik J G, Worsnop D R, Davidovits P, Jimenez J L (2004). Particle morphology and density characterization by combined mobility and aerodynamic diameter measurements. Part 1: theory. Aerosol Science and Technology, 38(12): 1185–1205

Deng C J, Fu Y Y, Dada L, Yan C, Cai R L, Yang D S, Zhou Y, Yin

R J, Lu Y Q, Li X X, et al. (2020). Seasonal characteristics of new particle formation and growth in urban Beijing. Environmental Science & Technology, 54(14): 8547–8557

Ding L, Zhang J B, Zheng H Y, Wang Y P, Fang L (2016). A method of simultaneously measuring particle shape parameter and aerodynamic size. Atmospheric Environment, 139: 87–97

Dong Z W, Qin D H, Li K M, Kang S C, Wei T, Lu J F (2019). Spatial variability, mixing states and composition of various haze particles in atmosphere during winter and summertime in northwest China. Environmental Pollution, 246: 79–88

Doubleday A, Blanco M N, Austin E, Marshall J D, Larson T V, Sheppard L (2023). Characterizing ultrafine particle mobile monitoring data for epidemiology. Environmental Science & Technology, 57(26): 9538–9547

Dutta M, Ghosh A, Sharma S K, Mandal T K, Chatterjee A (2023). CCN activation of ultrafine biogenic-WSOC under restricted anthropogenic emissions: a study over eastern Himalaya in India. Atmospheric Research, 287: 106704

Edebeli J, Spirig C, Fluck S, Fierz M, Anet J (2023). Spatiotemporal heterogeneity of lung-deposited surface area in zurich switzerland: lung-deposited surface area as a new routine metric for ambient particle monitoring. International Journal of Public Health, 68: 1605879

European Parliament & Council of the European Union (2024). Directive (EU) 2024/2881 of the European Parliament and of the Council of 23 October 2024 on ambient air quality and cleaner air for Europe. Official Journal of the European Union. Luxembourg: Publications Office of the European Union

Fajardo O A, Jiang J K, Hao J M (2016). Continuous measurement of ambient aerosol liquid water content in Beijing. Aerosol and Air Quality Research, 16(5): 1152–1164

Farina F, Lonati E, Milani C, Massimino L, Ballarini E, Donzelli E, Crippa L, Marmiroli P, Botto L, Corsetto P A, et al. (2019). *In vivo* comparative study on acute and sub-acute biological effects induced by ultrafine particles of different anthropogenic sources in BALB/c mice. International Journal of Molecular Sciences, 20(11): 2805

Fierz M, Houle C, Steigmeier P, Burtscher H (2011). Design, calibration, and field performance of a miniature diffusion size classifier. Aerosol Science and Technology, 45(1): 1–10

Fissan H, Neumann S, Trampe A, Pui D Y H, Shin W G (2007). Rationale and principle of an instrument measuring lung deposited nanoparticle surface area. Journal of Nanoparticle Research, 9(1): 53–59

Flagan R C (1998). History of electrical aerosol measurements. Aerosol Science and Technology, 28(4): 301–380

Fuchs N A (1963). On the stationary charge distribution on aerosol particles in a bipolar ionic atmosphere. Geofisica Pura e Applicata, 56(1): 185–193

Gani S, Chambliss S E, Messier K P, Lunden M M, Apte J S (2021). Spatiotemporal profiles of ultrafine particles differ from other traffic-related air pollutants: lessons from long-term measurements at fixed sites and mobile monitoring. Environmental Science: Atmospheres, 1(7): 558–568

Gao D, Ripley S, Weichenthal S, Godri Pollitt K J (2020). Ambient particulate matter oxidative potential: chemical determinants, associated health effects, and strategies for risk management. Free Radical Biology and Medicine, 151: 7–25

Garcia-Marlès M, Lara R, Reche C, Pérez N, Tobías A, Savadkoohi M, Beddows D, Salma I, Vörösmarty M, Weidinger T, et al. (2024). Inter-annual trends of ultrafine particles in urban Europe. Environment International, 185: 108510

Georgiades P, Kohl M, Nicolaou M A, Christoudias T, Pozzer A, Dovrolis C, Lelieveld J (2025). Global high-resolution ultrafine particle number concentrations through data fusion with machine learning. Scientific Data, 12(1): 1790

Gong J C, Zhu T, Hu M, Wu Z J, Zhang J F (2019). Different metrics (number, surface area, and volume concentration) of urban particles with varying sizes in relation to fractional exhaled nitric oxide (FeNO). Journal of Thoracic Disease, 11(4): 1714–1726

Gu X J, Peng Y, Tang X F, Wen Z Y, Lin X X, Li X Y, Hu Q Y, Wang J, Zhang W J (2025). Aerosol particle effective density of heated tobacco products measured with a tandem mass and mobility analyzer. Journal of Aerosol Science, 187: 106585

Gunn R, Woessner R H (1956). Measurements of the systematic electrification of aerosols. Journal of Colloid Science, 11(3): 254–259

Haul R (1982). S. J. Gregg, K. S. W. Sing: *Adsorption, Surface Area and Porosity*. 2. Auflage, Academic Press, London 1982. 303 Seiten, Preis: $ 49.50. Berichte der Bunsengesellschaft für Physikalische Chemie, 86(10): 957.

Hering S V, Stolzenburg M R (1995). On-line determination of particle size and density in the nanometer size range. Aerosol Science and Technology, 23(2): 155–173

Hinds W C, Zhu Y F (2022). Aerosol Technology: Properties, Behavior, and Measurement of Airborne Particles. Hoboken: John Wiley & Sons

Hoek G, Beelen R, De Hoogh K, Vienneau D, Gulliver J, Fischer P, Briggs D (2008). A review of land-use regression models to assess spatial variation of outdoor air pollution. Atmospheric Environment, 42(33): 7561–7578

Hu W W, Hu M, Hu W, Jimenez J L, Yuan B, Chen W T, Wang M, Wu Y S, Chen C, Wang Z B, et al. (2016). Chemical composition, sources, and aging process of submicron aerosols in Beijing: contrast between summer and winter. Journal of Geophysical Research: Atmospheres, 121(4): 1955–1977

ICRP (1994). International Commission on Radiological Protection Publication 66: Human Respiratory Tract Model for Radiological Protection. Oxford: Pergamon Press

Iida K, Sakurai H (2018). Counting efficiency evaluation of optical particle counters in micrometer range by using an inkjet aerosol generator. Aerosol Science and Technology, 52(10): 1156–1166

Iida K, Stolzenburg M R, McMurry P H (2009). Effect of working fluid on sub-2 nm particle detection with a laminar flow ultrafine condensation particle counter. Aerosol Science and Technology,

43(1): 81–96

Jeng H A (2010). Chemical composition of ambient particulate matter and redox activity. Environmental Monitoring and Assessment, 169(1−4): 597–606

Jiang J K, Chen M D, Kuang C, Attoui M, Mcmurry P H (2011). Electrical mobility spectrometer using a diethylene glycol condensation particle counter for measurement of aerosol size distributions down to 1 nm. Aerosol Science and Technology, 45(4): 510–521

Jiang J K, Kim C, Wang X L, Stolzenburg M R, Kaufman S L, Qi C L, Sem G J, Sakurai H, Hama N, McMurry P H (2014). Aerosol charge fractions downstream of six bipolar chargers: effects of ion source, source activity, and flowrate. Aerosol Science and Technology, 48(12): 1207–1216

Jiang J K, Oberdörster G, Biswas P (2009). Characterization of size, surface charge, and agglomeration state of nanoparticle dispersions for toxicological studies. Journal of Nanoparticle Research, 11(1): 77–89

Jiang J K, Oberdörster G, Elder A, Gelein R, Mercer P, Biswas P P (2008). Does nanoparticle activity depend upon size and crystal phase?. Nanotoxicology, 2(1): 33–42

Jianyao Y D, Yuan H Y, Su G F, Wang J, Weng W G, Zhang X L (2025). Machine learning-enhanced high-resolution exposure assessment of ultrafine particles. Nature Communications, 16(1): 1209

Jones R R, Hoek G, Fisher J A, Hasheminassab S, Wang D B, Ward M H, Sioutas C, Vermeulen R, Silverman D T (2020). Land use regression models for ultrafine particles, fine particles, and black carbon in Southern California. Science of the Total Environment, 699: 134234

Jung C H, Han K M, Yoon Y J, Kim D, Lee J Y, Lee H M, Um J, Lee S S, Kim Y P (2023a). Parameterization of polydisperse aerosol optical properties during hygroscopic growth. Aerosol Science and Technology, 57(8): 713–726

Jung C R, Chen W T, Young L H, Hsiao T C (2023b). A hybrid model for estimating the number concentration of ultrafine particles based on machine learning algorithms in central Taiwan. Environment International, 175: 107937

Kaye P H, Alexander-Buckley K, Hirst E, Saunders S, Clark J M (1996). A real-time monitoring system for airborne particle shape and size analysis. Journal of Geophysical Research: Atmospheres, 101(D14): 19215–19221

Kerckhoffs J, Hoek G, Gehring U, Vermeulen R (2021). Modelling nationwide spatial variation of ultrafine particles based on mobile monitoring. Environment International, 154: 106569

Kerckhoffs J, Hoek G, Messier K P, Brunekreef B, Meliefste K, Klompmaker J O, Vermeulen R (2016). Comparison of ultrafine particle and black carbon concentration predictions from a mobile and short-term stationary land-use regression model. Environmental Science & Technology, 50(23): 12894–12902

Kerckhoffs J, Hoek G, Vlaanderen J, Van Nunen E, Messier K, Brunekreef B, Gulliver J, Vermeulen R (2017). Robustness of intra urban land-use regression models for ultrafine particles and black carbon based on mobile monitoring. Environmental Research, 159: 500–508

Kirpes R M, Rodriguez B, Kim S, China S, Laskin A, Park K, Jung J, Ault A P, Pratt K A (2020). Emerging investigator series: influence of marine emissions and atmospheric processing on individual particle composition of summertime Arctic aerosol over the Bering Strait and Chukchi Sea. Environmental Science: Processes & Impacts, 22(5): 1201–1213

Kivekäs N, Sun J, Zhan M, Kerminen V M, Hyvärinen A, Komppula M, Viisanen Y, Hong N, Zhang Y, Kulmala M, et al. (2009). Long term particle size distribution measurements at Mount Waliguan, a high-altitude site in inland China. Atmospheric Chemistry and Physics, 9(15): 5461–5474

Konstandopoulos A G, Zarvalis D, Papaioannou E, Vlachos N D, Boretto G, Pidria M F, Faraldi P, Piacenza O, Prenninger P, Cartus T, et al. (2004). The Diesel Exhaust Aftertreatment (DEXA) Cluster: A Systematic Approach to Diesel Particulate Emission Control in Europe. SAE 2004 World Congress & Exhibition, Detroit, Michigan, USA

Kurihara K, Iwata A, Murray Horwitz S G, Ogane K, Sugioka T, Matsuki A, Okuda T (2022). Contribution of physical and chemical properties to dithiothreitol-measured oxidative potentials of atmospheric aerosol particles at urban and rural sites in Japan. Atmosphere, 13(2): 319

Kuula J, Kuuluvainen H, Niemi J V, Saukko E, Portin H, Kousa A, Aurela M, Rönkkö T, Timonen H (2020). Long-term sensor measurements of lung deposited surface area of particulate matter emitted from local vehicular and residential wood combustion sources. Aerosol Science and Technology, 54(2): 190–202

Lei T, Xiang W, Zhao B, Hou C Y, Ge M F, Wang W G (2024). Advances in analysis of atmospheric ultrafine particles and application in air quality, climate, and health research. Science of the Total Environment, 949: 175045

Li X X, Cai R L, Hao J M, Smith J N, Jiang J K (2023a). Online detection of airborne nanoparticle composition with mass spectrometry: recent advances, challenges, and opportunities. TrAC Trends in Analytical Chemistry, 166: 117195

Li X X, Chen Y J, Li Y Y, Cai R L, Li Y R, Deng C J, Wu J, Yan C, Cheng H R, Liu Y C, et al. (2023b). Seasonal variations in composition and sources of atmospheric ultrafine particles in urban Beijing based on near-continuous measurements. Atmospheric Chemistry and Physics, 23(23): 14801–14812

Li X X, Li Y Y, Cai R L, Yan C, Qiao X H, Guo Y S, Deng C J, Yin R J, Chen Y J, Li Y R, et al. (2022a). Insufficient condensable organic vapors lead to slow growth of new particles in an urban environment. Environmental Science & Technology, 56(14): 9936–9946

Li Y R, Chen X T, Jiang J K (2022b). Measuring size distributions of atmospheric aerosols using natural air ions. Aerosol Science and Technology, 56(7): 655–664

Li Y R, Chen X T, Wu J, Zhang Q, Zhang Z Z, Hao J M, Jiang J K (2025). A convertible condensation particle counter using alcohol or water as the working fluid. Aerosol Science and Technology,

59(2): 185–194

Li Y R, Wu J, Wu H, Liu X M, Zhou Q, Lu Y Q, Wu Y H, Liu M Y, Ou H J, Mai S X, et al. (2024). A bipolar SMPS network for measuring atmospheric aerosols using natural air ions. Atmospheric Environment, 325: 120462

Lin T C, Chiueh P T, Hsiao T C (2025). Challenges in observation of ultrafine particles: addressing estimation miscalculations and the necessity of temporal trends. Environmental Science & Technology, 59(1): 565–577

Liu Z W, Li H, Tang J, Wang M, Zheng H T, Luo T, Song X Q, Liu C F, Wang G C, Qin X F, et al. (2024). Multi-process atmospheric particle number size distribution over the Bohai Sea: insights from cruise and onboard unmanned aerial vehicle observations. Atmospheric Environment, 335: 120726

Lloyd M, Ganji A, Xu J S, Venuta A, Simon L, Zhang M Q, Saeedi M, Yamanouchi S, Apte J, Hong K, et al. (2023). Predicting spatial variations in annual average outdoor ultrafine particle concentrations in Montreal and Toronto, Canada: integrating land use regression and deep learning models. Environment International, 178: 108106

Lloyd M, Olaniyan T, Ganji A, Xu J S, Simon L, Zhang M Q, Saeedi M, Yamanouchi S, Wang A, Burnett R T, et al. (2024). Airborne ultrafine particle concentrations and brain cancer incidence in Canada's two largest cities. Environment International, 193: 109088

Lv L L, Wei P, Li J, Hu J N (2021). Application of machine learning algorithms to improve numerical simulation prediction of $PM_{2.5}$ and chemical components. Atmospheric Pollution Research, 12(11): 101211

Lv L P, Chen Y H, Zhao B (2024). Pathogen shape: implication on pathogenicity via respiratory deposition. Environment International, 191: 108978

Lv L P, Zhao B (2025). From shape to behavior: a synthesis of non-spherical particle dynamics in air. Particuology, 96: 218–243

Manninen H E, Mirme S, Mirme A, Petäjä T, Kulmala M (2016). How to reliably detect molecular clusters and nucleation mode particles with Neutral cluster and Air Ion Spectrometer (NAIS). Atmospheric Measurement Techniques, 9(8): 3577–3605

McMurry P H (2000a). The history of condensation nucleus counters. Aerosol Science and Technology, 33(4): 297–322

McMurry P H (2000b). A review of atmospheric aerosol measurements. Atmospheric Environment, 34(12−14): 1959–1999

Mills J B, Park J H, Peters T M (2013). Comparison of the DiSCmini aerosol monitor to a handheld condensation particle counter and a scanning mobility particle sizer for submicrometer sodium chloride and metal aerosols. Journal of Occupational and Environmental Hygiene, 10(5): 250–258

Morawska L, Wang H, Ristovski Z, Jayaratne E R, Johnson G, Cheung H C, Ling X, He C (2009). JEM Spotlight: environmental monitoring of airborne nanoparticles. Journal of Environmental Monitoring, 11(10): 1758–1773

Moreno-Ríos A L, Tejeda-Benítez L P, Bustillo-Lecompte C F (2022). Sources, characteristics, toxicity, and control of ultrafine particles: an overview. Geoscience Frontiers, 13(1): 101147

Ning Z, Chan K L, Wong K C, Westerdahl D, Močnik G, Zhou J H, Cheung C S (2013). Black carbon mass size distributions of diesel exhaust and urban aerosols measured using differential mobility analyzer in tandem with Aethalometer. Atmospheric Environment, 80: 31–40

Nordmann S, Birmili W, Weinhold K, Wiedensohler A, Mertes S, Mueller K, Gnauk T, Herrmann H, Pitz M, Cyrys J, et al. (2009). Atmospheric aerosol measurements in the German Ultrafine Aerosol Network (GUAN). Gefahrstoffe, Reinhaltung der Luft / Air Quality Control, 69(11−12): 469–474

Oxford C R, Rapp C M, Wang Y, Kumar P, Watson D, Portelli J L, Sussman E A, Dhawan S, Jiang J K, Williams B J (2019). Development and qualification of a VH-TDMA for the study of pure aerosols. Aerosol Science and Technology, 53(2): 120–132

Pietrogrande M C, Romanato L, Russo M (2022). Synergistic and antagonistic effects of aerosol components on its oxidative potential as predictor of particle toxicity. Toxics, 10(4): 196

Pongetti J, Nickolaus C, Symonds J P R (2022). Using the Aerodynamic Aerosol Classifier (AAC) as a Low-pass Separator. 11th International Aerosol Conference 2022, Athens, Greece

Rader D J, McMurry P H (1986). Application of the tandem differential mobility analyzer to studies of droplet growth or evaporation. Journal of Aerosol Science, 17(5): 771–787

Rahman M, Karunasinghe J, Clifford S, Knibbs L D, Morawska L (2020). New insights into the spatial distribution of particle number concentrations by applying non-parametric land use regression modelling. Science of the Total Environment, 702: 134708

Reggente M, Peters J, Theunis J, Van Poppel M, Rademaker M, Kumar P, De Baets B (2014). Prediction of ultrafine particle number concentrations in urban environments by means of Gaussian process regression based on measurements of oxides of nitrogen. Environmental Modelling & Software, 61: 135–150

Riva M, Rantala P, Krechmer J E, Peräkylä O, Zhang Y J, Heikkinen L, Garmash O, Yan C, Kulmala M, Worsnop D, et al. (2019). Evaluating the performance of five different chemical ionization techniques for detecting gaseous oxygenated organic species. Atmospheric Measurement Techniques, 12(4): 2403–2421

Sakurai H, Fink M A, McMurry P H, Mauldin L, Moore K F, Smith J N, Eisele F L (2005). Hygroscopicity and volatility of 4–10 nm particles during summertime atmospheric nucleation events in urban Atlanta. Journal of Geophysical Research: Atmospheres, 110(D22): D22S04

Saleh Y, Antherieu S, Dusautoir R, Alleman L Y, Sotty J, De Sousa C, Platel A, Perdrix E, Riffault V, Fronval I, et al. (2019). Exposure to atmospheric ultrafine particles induces severe lung inflammatory response and tissue remodeling in mice. International Journal of Environmental Research and Public Health, 16(7): 1210

Sardar S B, Fine P M, Mayo P R, Sioutas C (2005). Size-fractionated measurements of ambient ultrafine particle chemical composition

in Los Angeles using the NanoMOUDI. Environmental Science & Technology, 39(4): 932–944

Schmid O, Stoeger T (2016). Surface area is the biologically most effective dose metric for acute nanoparticle toxicity in the lung. Journal of Aerosol Science, 99: 133–143

Seinfeld J H, Pandis S N (2016). Atmospheric Chemistry and Physics: From Air Pollution to Climate Change. 3rd ed. Hoboken: Wiley

Smith J N, Moore K F, Mcmurry P H, Eisele F L (2004). Atmospheric measurements of sub-20 nm diameter particle chemical composition by thermal desorption chemical ionization mass spectrometry. Aerosol Science and Technology, 38(2): 100–110

Steffens J, Kimbrough S, Baldauf R, Isakov V, Brown R, Powell A, Deshmukh P (2017). Near-port air quality assessment utilizing a mobile measurement approach. Atmospheric Pollution Research, 8(6): 1023–1030

Stokes R H, Robinson R A (1966). Interactions in aqueous nonelectrolyte solutions. I. Solute-solvent equilibria. The Journal of Physical Chemistry, 70(7): 2126–2131

Sun J, Birmili W, Hermann M, Tuch T, Weinhold K, Spindler G, Schladitz A, Bastian S, Löschau G, Cyrys J, et al. (2019). Variability of black carbon mass concentrations, sub-micrometer particle number concentrations and size distributions: results of the German Ultrafine Aerosol Network ranging from city street to High Alpine locations. Atmospheric Environment, 202: 256–268

Tammet H, Mirme A, Tamm E (2002). Electrical aerosol spectrometer of Tartu University. Atmospheric Research, 62(3−4): 315–324

Tavakoli F, Olfert J S (2013). An instrument for the classification of aerosols by particle relaxation time: theoretical models of the aerodynamic aerosol classifier. Aerosol Science and Technology, 47(8): 916–926

Tigges L, Jain A, Schmid H J (2015). On the bipolar charge distribution used for mobility particle sizing: theoretical considerations. Journal of Aerosol Science, 88: 119–134

Vachon J, Buteau S, Liu Y, Van Ryswyk K, Hatzopoulou M, Smargiassi A (2024a). Spatial and spatiotemporal modelling of intra-urban ultrafine particles: a comparison of linear, nonlinear, regularized, and machine learning methods. Science of the Total Environment, 954: 176523

Vachon J, Kerckhoffs J, Buteau S, Smargiassi A (2024b). Do machine learning methods improve prediction of ambient air pollutants with high spatial contrast? A systematic review. Environmental Research, 262(Pt 2): 119751

Vasilatou K, Wälchli C, Koust S, Horender S, Iida K, Sakurai H, Schneider F, Spielvogel J, Wu T Y, Auderset K (2021). Calibration of optical particle size spectrometers against a primary standard: counting efficiency profile of the TSI Model 3330 OPS and Grimm 11-D monitor in the particle size range from 300 nm to 10 μm. Journal of Aerosol Science, 157: 105818

Venzac H, Sellegri K, Laj P, Villani P, Bonasoni P, Marinoni A, Cristofanelli P, Calzolari F, Fuzzi S, Decesari S, et al. (2008). High frequency new particle formation in the Himalayas. Proceedings of the National Academy of Sciences of the United States of America, 105(41): 15666–15671

Villani P, Picard D, Michaud V, Laj P, Wiedensohler A (2008). Design and validation of a volatility hygroscopic tandem differential mobility analyzer (VH-TDMA) to characterize the relationships between the thermal and hygroscopic properties of atmospheric aerosol particles. Aerosol Science and Technology, 42(9): 729–741

Voth G A, Soldati A (2017). Anisotropic particles in turbulence. Annual Review of Fluid Mechanics, 49: 249–276

Vu T V, Delgado-Saborit J M, Harrison R M (2015). A review of hygroscopic growth factors of submicron aerosols from different sources and its implication for calculation of lung deposition efficiency of ambient aerosols. Air Quality, Atmosphere & Health, 8(5): 429–440

Wadell H (1932). Volume, shape, and roundness of rock particles. The Journal of Geology, 40(5): 443–451

Wang W Y, Zhao X, Zhang J S, Yang Y X, Yu T Z, Bian J J, Gui H Q, Liu J G (2020). Design and evaluation of a condensation particle counter with high performance for single-particle counting. Instrumentation Science & Technology, 48(2): 212–229

Wehner B, Siebert H, Ansmann A, Ditas F, Seifert P, Stratmann F, Wiedensohler A, Apituley A, Shaw R A, Manninen H E, et al. (2010). Observations of turbulence-induced new particle formation in the residual layer. Atmospheric Chemistry and Physics, 10(9): 4319–4330

Weichenthal S, Farrell W, Goldberg M, Joseph L, Hatzopoulou M (2014). Characterizing the impact of traffic and the built environment on near-road ultrafine particle and black carbon concentrations. Environmental Research, 132: 305–310

Weimer S, Mohr C, Richter R, Keller J, Mohr M, Prévôt A S H, Baltensperger U (2009). Mobile measurements of aerosol number and volume size distributions in an Alpine valley: influence of traffic versus wood burning. Atmospheric Environment, 43(3): 624–630

Whitby K T (1978). The physical characteristics of sulfur aerosols. Atmospheric Environment (1967), 12(1−3): 135–159

WHO (2021). WHO global air quality guidelines: particulate matter ($PM_{2.5}$ and PM_{10}), ozone, nitrogen dioxide, sulfur dioxide and carbon monoxide. Geneva: World Health Organization

Wiedensohler A (1988). An approximation of the bipolar charge distribution for particles in the submicron size range. Journal of Aerosol Science, 19(3): 387–389

Wiedensohler A, Birmili W, Nowak A, Sonntag A, Weinhold K, Merkel M, Wehner B, Tuch T, Pfeifer S, Fiebig M, et al. (2012). Mobility particle size spectrometers: harmonization of technical standards and data structure to facilitate high quality long-term observations of atmospheric particle number size distributions. Atmospheric Measurement Techniques, 5(3): 657–685

Wiedensohler A, Lütkemeier E, Feldpausch M, Helsper C (1986).

Investigation of the bipolar charge distribution at various gas conditions. Journal of Aerosol Science, 17(3): 413–416

Wiedensohler A, Wiesner A, Weinhold K, Birmili W, Hermann M, Merkel M, Müller T, Pfeifer S, Schmidt A, Tuch T, et al. (2018). Mobility particle size spectrometers: calibration procedures and measurement uncertainties. Aerosol Science and Technology, 52(2): 146–164

WMO (2016). WMO/GAW Aerosol Measurement Procedures, Guidelines and Recommendations (2nd ed.). GAW Report No. 227. Geneva: World Meteorological Organization

Wu C A, Chen Y T, Young L H, Chang P K, Chou L T, Chen A Y, Hsiao T C (2023). Ultrafine particles in urban settings: a combined study of volatility and effective density revealed by VT-DMA-APM. Atmospheric Environment, 312: 120054

Xu J S, Zhang M Q, Ganji A, Mallinen K, Wang A, Lloyd M, Venuta A, Simon L, Kang J, Gong J, et al. (2022). Prediction of short-term ultrafine particle exposures using real-time street-level images paired with air quality measurements. Environmental Science & Technology, 56(18): 12886–12897

Ye Q, Li H Z, Gu P S, Robinson E S, Apte J S, Sullivan R C, Robinson A L, Donahue N M, Presto A A (2020). Moving beyond fine particle mass: high-spatial resolution exposure to source-resolved atmospheric particle number and chemical mixing state. Environmental Health Perspectives, 128(1): 017009

Zahir M Z, Akhtar K, Yook S J (2025). Enhancing electric virtual impactor performance with condensational growth and efficient charging for size-selective sampling of fine and ultrafine particles. Advanced Powder Technology, 36(8): 104972

Zarrin F, Risfelt J A, Dovichi N J (1987). Light scatter detection within the sheath flow cuvette for size determination of multicomponent submicrometer particle suspensions. Analytical Chemistry, 59(6): 850–854

Zdanovskij A B (1936). Zakonomernosti v izmeneniâh svojstv smešannyh rastvorov. Moscow; Leningrad: Izd. THAN USSR

Zhang Y R, Han Y (2025a). Direct measurement techniques for atmospheric aerosol: optical and chemical properties review. Science China Earth Sciences, 68(11): 3454–3481

Zhang Y R, Han Y (2025b). Direct measurement techniques for atmospheric aerosol: physical properties review. Atmospheric Environment, 344: 121034

Zhao P S, Du X, Su J, Ding J, Dong Q (2020). Aerosol hygroscopicity based on size-resolved chemical compositions in Beijing. Science of the Total Environment, 716: 137074

Zou S J, Chen L, Xu H H, Zhang R, Liu M Y, Liu G Q, Ye J H, Yang H L, Wu H, Yang Y S, et al. (2025). Observed size-dependent effect of the marine air on aerosols hygroscopicity at a coastal site of Shenzhen, China. Atmospheric Research, 315: 107830